

Molecular models for cyclic alkanes and ethyl acetate as well as surface tension data from molecular simulation

Stefan Eckelsbach¹, Tatjana Janzen¹, Andreas Köster¹, Svetlana Miroshnichenko¹, Yonny Mauricio Muñoz-Muñoz¹, and Jadran Vrabec¹

1 Introduction

Thermodynamic data for most technically interesting systems are still scarce or even unavailable despite the large experimental effort that was invested over the last century into their measurement. This particularly applies to mixtures containing two or more components and systems under extreme conditions. In contrast to phenomenological methods, molecular modeling and simulation is based on a sound physical foundation and is therefore well suited for the prediction of such properties and processes.

In this work new molecular force field models, i.e. for four cyclic alkanes and ethyl acetate, are presented to widen the application area of molecular simulation.

In the second part of this work vapor-liquid interfaces were investigated, deepening the understanding of interfacial processes of a model fuel, consisting of acetone, nitrogen and oxygen, similar to the state of injected acetone droplets in a gaseous fluid in combustion chambers.

In the third part an efficient method for the generation of large simulation data sets is studied with respect to the stability and accuracy, using the microcanonical ensemble (*NVE*) instead of the canonic (*NVT*) ensemble.

2 Optimization of potential models for cyclic alkanes from cyclopropane to cyclohexane

Cyclic hydrocarbons are substances that are very common in the chemical industry, having one or more rings in their molecular structure. Cyclic alkanes with a single

¹ Lehrstuhl für Thermodynamik und Energietechnik (ThEt), Universität Paderborn, Warburger Str. 100, 33098 Paderborn · Author to whom correspondence should be addressed: J. Vrabec, e-mail: jadran.vrabec@upb.de.

ring are part of this class of compounds and can be represented with the general molecular formula C_nH_{2n} . These compounds, that are primarily found in crude oil, have single bonds between the carbon atoms, i.e. their carbon atoms are completely saturated.

In the petrochemical industry, for example, cyclohexane is produced from the hydrogenation of benzene, albeit the inverse reaction, i.e. the dehydrogenation of cyclohexane to yield benzene is more important. An improvement of the understanding of the nature of all involved physical forces of the cyclic alkanes may lead to various technical applications, including chemical equilibrium studies and vapor-liquid equilibrium (VLE) data extraction for both pure substances and mixtures. Furthermore, both temperature and pressure can be obtained using molecular simulations to study the development of hydrates, which is important since their formation e.g. causes obstructions of pipes.

Moreover, it is believed that with accurate potential models it will be possible to obtain hybrid models which might decrease experimental effort and costs. Scarce experimental data are available for cyclobutane, such that molecular simulation can be a source to provide pseudo experimental data and can contribute to extend existing models. Thus the motivation is to develop accurate molecular force field models for these substances, which constitutes the principal objective of this work.

The parameterization route introduced in prior work of our group [1] was adapted in this work, to obtain accurate intermolecular potential models from cyclopropane (C_3H_6) to cyclohexane (C_6H_{12}). To obtain such potential models, the cycloalkane molecules were assumed to be rigid, i.e. without internal degrees of freedom, formed by Lennard-Jones (LJ) sites bonded in a ring shaped structure with internal angles computed by quantum mechanical calculations.

The geometric structure of all molecules was obtained with the open source code for computational chemistry calculations GAMESS (US) [2], using the Hartree-Fock (HF) method with a relatively small (6-31 G) basis set. Thereby all atomic positions were determined for each hydrogen and carbon atom in the molecule. Cyclopropane is an essentially planar molecule, characterized only by bond angles and bond lengths. This is in contrast to cyclobutane, cyclopentane and cyclohexane, which require the specification of dihedral angles due to their three-dimensional structure.

A reduction of computational costs can be achieved by employing the united atoms approximation, whereby the methylene group is represented by a single methylene site. The LJ force centre for each methylene site was initially located at the position of the carbon atom, as determined by the HF method.

Subsequently, the methylene site-site distance was gradually modified while keeping the bond and dihedral angles invariant, molecular simulation runs were performed to compute VLE data for the pure substances using the *ms2* code [3] and the LJ parameters reported by [1]. The procedure was repeated for all molecules studied in this work.

The simulation results were compared to experimental data for the VLE properties, the critical point and second virial coefficient from the literature. Whenever reasonable results were obtained for VLE properties, such as saturated liquid den-

sity, vapor pressure and enthalpy of vaporization, the methylene site-site distances were fixed and the models were then subject to further optimization.

The LJ parameters were optimized using the reduced method by Merker et al. [4], which constitutes a computationally effective procedure, since no additional molecular simulation runs are necessary.

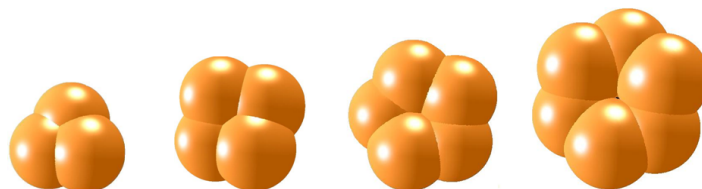


Fig. 1 Snapshots of cyclopropane (C_3H_6), cyclobutane (C_4H_8), cyclopentane (C_5H_{10}) and cyclohexane (C_6H_{12}) obtained in this work (left to right)

Figure 1 shows a snapshot for each molecular structure obtained in this work. Every geometry contains the internal angles as computed by quantum mechanical calculations, but the site-site distances were enlarged. The cyclopropane structure was planar, while the cyclobutane and cyclopentane are three-dimensional structures. For the cyclohexane case, the chair configuration was chosen.

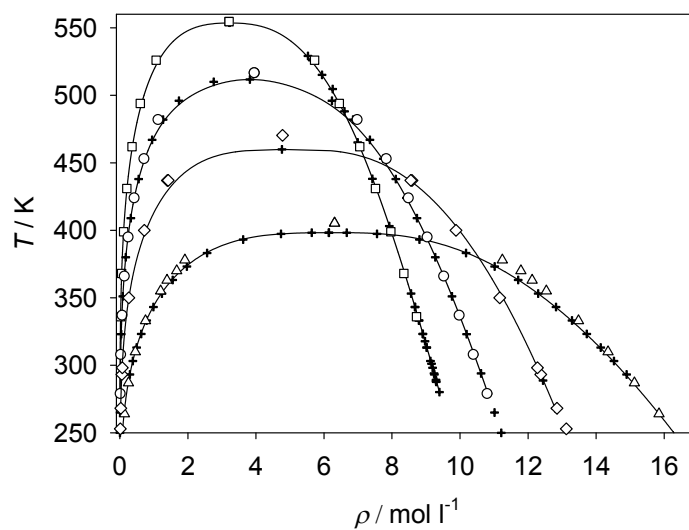


Fig. 2 Vapor-liquid envelopes of the cycloalkanes studied in this work. Triangles represent C_3H_6 , diamonds C_4H_8 , circles C_5H_{10} and squares C_6H_{12} . The cross symbol corresponds to experimental data from the literature.

Figure 2 shows the molecular simulation results for the VLE for each fluid studied in this work, including the critical point. The continuous lines are the data from the best reference equations of state that are available for cyclopentane and cyclohexane. For the cyclopropane and cyclobutane cases, the continuous lines are data from typical correlations that are used in the literature. Moreover, experimental data are shown for each fluid. Note that for the cyclobutane case, the experimental data are very scarce, but molecular simulation results have similar performance as the DIPPR [5] correlations.

3 Ethyl acetate

Ethyl acetate is the organic compound with the formula $\text{CH}_3 - \text{COO} - \text{CH}_2 - \text{CH}_3$. It is produced by the esterification reaction of ethanol and acetic acid and is synthesized on a large scale for a use as a solvent. VLE data are necessary for the design and optimization of separation processes, therefore, a new molecular model for ethyl acetate is proposed here.

3.1 Molecular model class

The present molecular model include three groups of potential parameters. These are the geometric parameters, specifying the positions of different interaction sites, the electrostatic parameters, defining the polar interactions in terms of point charges, dipoles or quadrupoles, and the dispersive and repulsive parameters, determining the attraction by London forces and the repulsion by electronic orbital overlaps. Here, the LJ 12-6 potential [6, 7] was used to describe the dispersive and repulsive interactions. The total intermolecular interaction energy thus writes as

$$U = \sum_{i=1}^{N-1} \sum_{j=i+1}^N \left\{ \sum_{a=1}^{S_i^{\text{LJ}}} \sum_{b=1}^{S_j^{\text{LJ}}} 4\epsilon_{ijab} \left[\left(\frac{\sigma_{ijab}}{r_{ijab}} \right)^{12} - \left(\frac{\sigma_{ijab}}{r_{ijab}} \right)^6 \right] + \sum_{c=1}^{S_i^e} \sum_{d=1}^{S_j^e} \frac{1}{4\pi\epsilon_0} \left[\frac{q_{ic}q_{jd}}{r_{ijcd}} + \frac{q_{ic}\mu_{jd} + \mu_{ic}q_{jd}}{r_{ijcd}^2} \cdot f_1(\boldsymbol{\omega}_i, \boldsymbol{\omega}_j) + \frac{q_{ic}Q_{jd} + Q_{ic}q_{jd}}{r_{ijcd}^3} \cdot f_2(\boldsymbol{\omega}_i, \boldsymbol{\omega}_j) + \frac{\mu_{ic}\mu_{jd}}{r_{ijcd}^3} \cdot f_3(\boldsymbol{\omega}_i, \boldsymbol{\omega}_j) + \frac{\mu_{ic}Q_{jd} + Q_{ic}\mu_{jd}}{r_{ijcd}^4} \cdot f_4(\boldsymbol{\omega}_i, \boldsymbol{\omega}_j) + \frac{Q_{ic}Q_{jd}}{r_{ijcd}^5} \cdot f_5(\boldsymbol{\omega}_i, \boldsymbol{\omega}_j) \right] \right\}, \quad (1)$$

where r_{ijab} , ϵ_{ijab} , σ_{ijab} are the distance, the LJ energy parameter and the LJ size parameter, respectively, for the pair-wise interaction between LJ site a on molecule i and LJ site b on molecule j . The permittivity of the vacuum is ϵ_0 , whereas q_{ic} , μ_{ic} and Q_{ic} denote the point charge magnitude, the dipole moment and the quadrupole

moment of the electrostatic interaction site c on molecule i and so forth. The expressions $f_x(\mathbf{w}_i, \mathbf{w}_j)$ stand for the dependence of the electrostatic interactions on the orientations \mathbf{w}_i and \mathbf{w}_j of the molecules i and j [8, 9]. Finally, the summation limits N , S_x^{LJ} and S_x^{e} denote the number of molecules, the number of LJ sites and the number of electrostatic sites, respectively. The atomic charges were estimated here by the Mulliken method [10].

Lorentz-Berthelot combining rules are used to determine cross-parameters for Lennard-Jones interactions between sites of different type [11, 12]:

$$\sigma_{ijab} = \frac{\sigma_{iiaa} + \sigma_{jjbb}}{2}, \quad (2)$$

and

$$\epsilon_{ijab} = \sqrt{\epsilon_{iiaa}\epsilon_{jjbb}}. \quad (3)$$

3.2 Molecular model of ethyl acetate

A new molecular model was developed for ethyl acetate based on quantum chemical (QC) information on molecular geometry and electrostatics. In a first step, the geometric data of the molecules, i.e. bond lengths, angles and dihedrals, were determined by QC calculations. Therefore, a geometry optimization was performed via an energy minimization using the GAMESS(US) package [2]. The Hartree-Fock level of theory was applied with a relatively small (6-31 G) basis set. Intermolecular electrostatic interactions mainly occur due to the static polarity of single molecules that can well be obtained by QC. Here, the Møller-Plesset 2 level of theory was used that considers electron correlation in combination with the polarizable 6-31G basis set.

Figure 3 shows the devised molecular model.

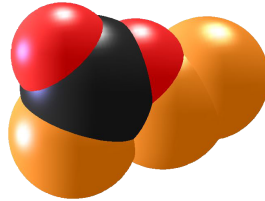


Fig. 3 Snapshot of ethyl acetate

The new model of ethyl acetate is based on the work of Kamath et al. [13], which is improved by including geometry and electrostatics from QM calculations. The initial model adopted the LJ parameters by Kamath et al., which were then adjusted to experimental VLE data, i.e. saturated liquid density, vapor pressure, and enthalpy of vaporization, until a desired quality was reached.

The present ethyl acetate model consists of six LJ sites (one for the methylene bridge, one for each oxygen atom, and one for each methyl group). The electrostatic interactions were modeled by five point charges. The parameters of the LJ sites were adjusted to experimental saturated liquid density and vapor pressure. The full parameter set of the new ethyl acetate model is listed in Table 1.

Table 1 Parameters of the molecular model for ethyl acetate developed in this work. Lennard-Jones interaction sites are denoted by the modeled atomic groups. Electrostatic interaction sites are denoted by point charge. Coordinates are given with respect to the center of mass in a principal axes system.

interaction site	x Å	y Å	z Å	σ Å	ϵ/k_B K	q e
CH ₃	-2.273	1.172	0	3.7227	74.139	
CH ₂	-1.312	0.018	0	3.9212	34.800	
O	0.000	0.589	0	3.0278	59.765	
C	1.101	-0.203	0	3.8716	31.018	
O	2.188	0.321	0	2.7796	41.609	
CH ₃	0.897	-1.690	0	3.7227	74.139	
point charge (CH ₂)	-1.312	0.018	0			0.306
point charge (O)	0.000	0.589	0			-0.474
point charge (C)	1.101	-0.203	0			0.593
point charge (O)	2.188	0.321	0			-0.415
point charge (CH ₃)	0.897	-1.690	0			-0.010

The pure substance VLE simulation results are shown in figures 4 and 5, where they are compared to experimental data and the DIPPR correlations [14]. The new ethyl acetate model shows mean unsigned deviations to experimental data of 0.1 % for the saturated liquid density, 4.6 % for the vapor pressure and 4.3 % for the enthalpy of vaporization over the whole temperature range from the triple point to the critical point.

For pure ethyl acetate, predicted data on the second virial coefficient is available from DIPPR. Figure 5 shows the simulation results compared to correlation of predicted data taken from DIPPR [14]. The present second virial coefficient agrees well with the DIPPR correlation at high temperatures, however at low temperatures, some noticeable deviations are present yielding a mean error of about 0.5 l/mol.

3.3 Binary vapor-liquid equilibria

Based on the devised molecular model of ethyl acetate, VLE data were predicted for the binary system ethyl acetate + chloroform. The molecular model for chloroform was taken from Stoll et al. [16] and is of the two-center LJ plus point dipole type. The vapor-liquid phase behavior of the binary mixture was predicted by molecular simulation and compared to experimental data as well as the Peng-Robinson equation of state [17].

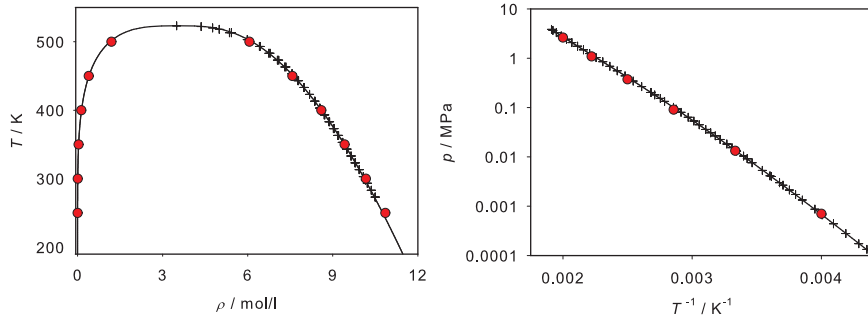


Fig. 4 Simulation results (●), experimental data [15] (+) and DIPPR correlation of experimental data [14] (—) of ethyl acetate. Left: saturated densities, right: vapor pressure. The statistical uncertainties of the present simulation data are within symbol size.

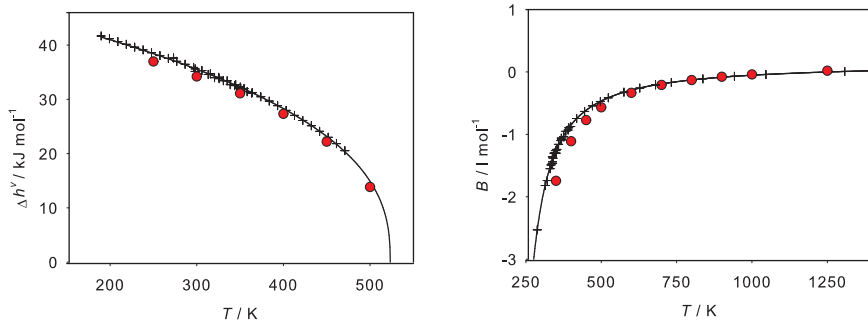


Fig. 5 Simulation results (●), experimental data [15] (+) and DIPPR correlation of experimental data [15] (—) of ethyl acetate. Left: enthalpy of vaporisation, right: second virial coefficient. The statistical uncertainties of the present simulation data are within symbol size.

Figure 6 shows the isothermal VLE of ethyl acetate + chloroform at 323.15 K from experiment [18], simulation and Peng-Robinson equation of state. The experimental vapor pressure at a liquid mole fraction of $x_{\text{chloroform}} = 0.5$ mol/mol was taken to adjust the binary parameter of the molecular model ($\xi = 1.04$) and of the Peng-Robinson equation of state ($k_{ij} = -0.085$). It can be seen that the results obtained by molecular simulation agree well with the experimental results and the Peng-Robinson equation of state.

4 Interfacial properties of binary mixtures

Interfacial properties are of interest for processes containing two or more phases, which is basically the default case for complex technical and natural systems, in-

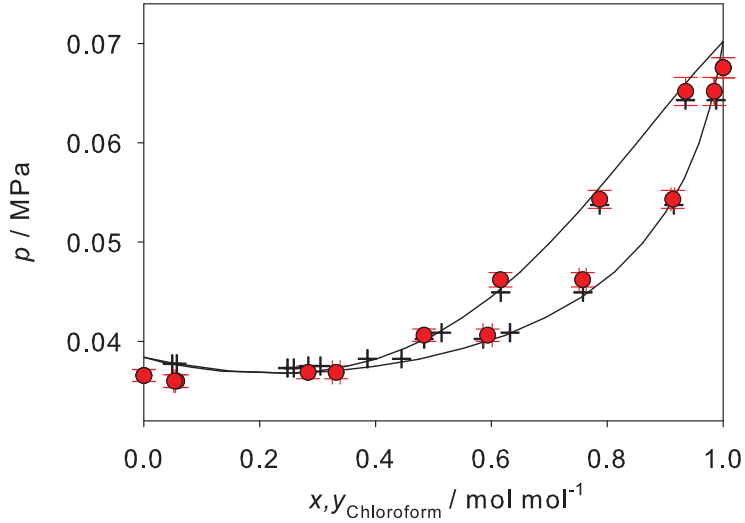


Fig. 6 Isothermal vapor-liquid phase diagram of ethyl acetate + chloroform at 323.15 K: present simulation data with $\xi = 1.04$ (●); experimental data by Ohta et al. [18] (+); Peng-Robinson equation of state with $k_{ij} = -0.085$ (—).

cluding separation processes, boiling and any system containing droplets. Many of these processes occur under extreme conditions of temperature or pressure, e.g. in case of flash boiling in combustion chambers. Such processes are actively being used although striking gaps remain in their essential understanding. At the same time, thermodynamic data for most technically interesting systems are still scarce or even unavailable despite the large experimental effort that was invested into their measurement. This particularly applies to mixtures of two or more components and systems under extreme conditions.

In this work, interfacial properties of the binary mixtures nitrogen + oxygen and nitrogen + acetone were investigated. These mixtures serve as a model fuel, yielding interfacial data and deepen the general understanding of the interfacial processes for the injection of acetone droplets in a gaseous fluid, consisting of nitrogen and oxygen. For this purpose, direct simulations of vapor-liquid equilibria were carried out, with particular attention to the interface region.

First, density and composition data of the bulk phases were required to set up the simulations. These data were obtained from simulations using the molecular simulation tool *ms2* [3]. Molecular force field models, adjusted to the mixtures with an additional binary interaction parameter, from previous works of our group were used [19, 20]. They lead to very good agreement with reference data even for temperatures near the critical point, typically having only a 2% deviation to the critical density ρ_c [20].

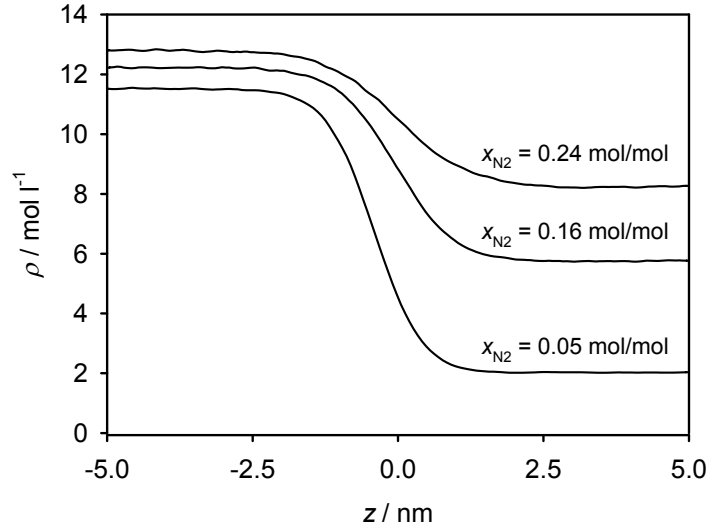


Fig. 7 Profile of the total density over the length of the simulation volume. The temperature is constant at 400 K. Three mixtures containing nitrogen and acetone are shown for three different compositions: the liquid mole fractions are $x_{N_2} = 0.05$ mol/mol, $x_{N_2} = 0.16$ mol/mol, and $x_{N_2} = 0.24$ mol/mol.

Further simulations were carried out with the highly parallel molecular dynamics code *ls1* [21]. Due to the inhomogeneity of the simulated systems, the long range correction of Janeček was used [22]. After an equilibration period, the interface region was formed, which gave the possibility for further investigation. The equilibrated states of the interface region are shown exemplarily in figure 7 for three different compositions at the constant temperature of 400 K.

The surface tension can be calculated following the Irving-Kirkwood approach [23]

$$\gamma = \frac{1}{2A} (2\Pi_{zz} - (\Pi_{xx} + \Pi_{yy})), \quad (4)$$

where A is the area of the interface and $\Pi_{\alpha\beta}$ is an element of the virial tensor, which is defined as

$$\Pi_{\alpha\beta} = \left\langle \frac{1}{2} \sum_{i=1}^N \sum_{j=1}^N r_{ij}^{\alpha} f_{ij}^{\beta} \right\rangle. \quad (5)$$

The indices α and β represent the x -, y - or z -directions of the distance vector r_{ij} and the force vector f_{ij} , in each case between molecules i and j . The virial tensor in normal ($\Pi_N = \Pi_{zz}$) and tangential direction ($\Pi_T = (\Pi_{xx} + \Pi_{yy})/2$) as well as the difference between these are exemplarily shown in figure 8 for one state point.

The simulated surface tension was compared to experimental data, which are relatively rare and only available for the pure substances. Thus the prediction of the

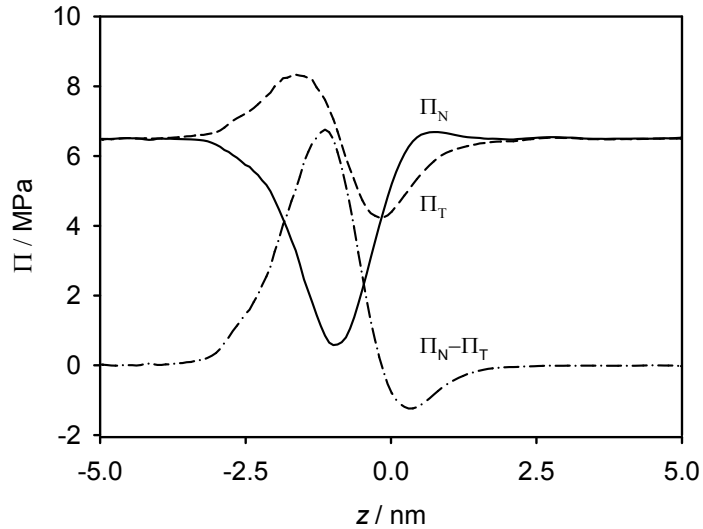


Fig. 8 Profile of the virial tensor over the length of the simulation volume. The virial tensor in normal direction Π_N , in tangential direction Π_T and the difference of these are shown. The mixture consists of nitrogen and acetone with a liquid mole fraction of $x_{N_2} = 0.05$ and a temperature of 400 K.

surface tension based on the parachor [29] was used for comparison with the results for the binary mixtures. In figure 9 the simulation results for the pure substances nitrogen and oxygen as well as their mixture are given. The mixture was set up in an equimolar state for the liquid phase. The simulation data for the pure substances are in good agreement with the surface tension correlation by Mulero et al. [25], which is based on experimental data, and the experimental data itself. In general, the direct simulations using the Monte Carlo scheme by Neyt et al. [24] show a slight overestimation in comparison with the reference data. The simulation results of the mixture nitrogen + oxygen also show a good agreement with the correlation [25]. The prediction following the parachor method is based on data calculated with the equations of state by Schmidt et al. [30] and Span et al. [31] and yields results, that are a little bit lower in the whole considered temperature range, but are relatively close to the reference.

In figure 10 the simulation results for the surface tension of the mixture nitrogen + acetone are plotted over the liquid mole fraction at 400 K and 450 K. For higher mole fractions near the critical point, the simulated data concur with the results of Klink and Gross (personal communication, 25 Feb 2014), determined by the density functional theory method. For smaller mole fractions, the simulation results are somewhat lower, until they match the correlation by Mulero et al. [25] for pure acetone within the estimated uncertainties of the present simulations. For this state the data by Klink and Gross overestimate the surface tension in comparison

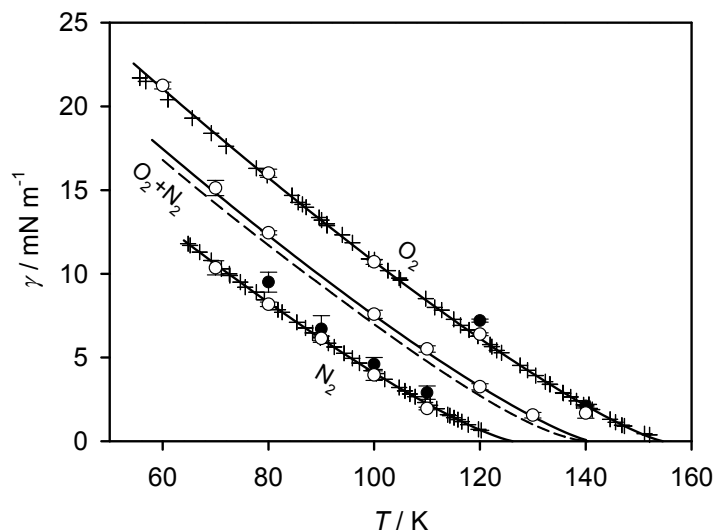


Fig. 9 Surface tension over temperature for the pure substances nitrogen and oxygen and their equimolar (liquid phase) mixture. Simulations: \circ this work, \bullet Neyt et al. [24]; correlations: — Mulero et al. [25], --- parachor method; experimental data: + [26, 27, 28]. The statistical uncertainties of the simulation data indicate the standard error on a 95 % confidence interval.

to the correlation of experimental data. Here the parachor method was based on the Peng-Robinson equation of state with the Huron-Vidal mixing rule, published by Windmann et al. [20]. Its results underestimate the surface tension significantly for both investigated temperatures. The parachor method strongly depends on the input data and is thus susceptible to their quality, which, of course, is better for the highly accurate and more complex equations of state by Schmidt et al. [30] and Span et al. [31].

5 Thermodynamic data by molecular simulations in the microcanonical ensemble

The importance of a solid base of thermodynamic data for the design and optimization of technological processes is crucial [32]. It was shown that molecular force field models allow for the generation of large and widespread data sets in a very short amount of time, due to the use of the molecular simulation framework proposed by Lustig [33], which gives access to any A_{mn}^r ($m, n > 0$) in the NVT ensemble for a specific state point through

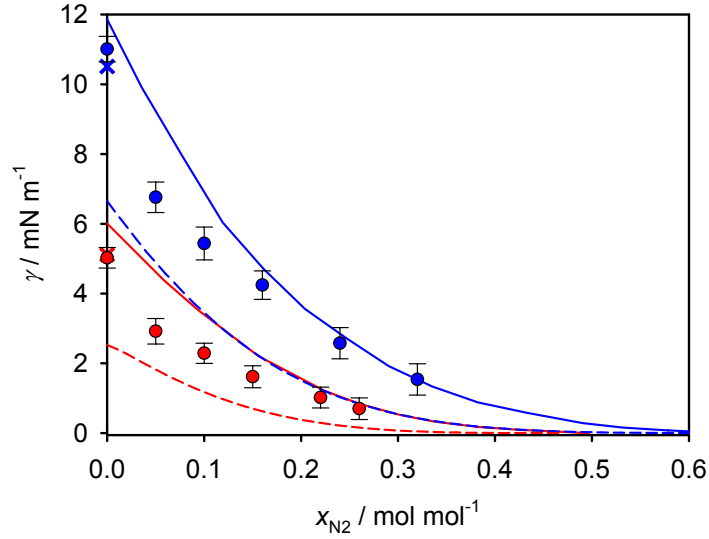


Fig. 10 Surface tension over liquid mole fraction of nitrogen for the mixture nitrogen and acetone at 400 K (blue) and 450 K (red), respectively. \circ molecular dynamics, this work, — density functional theory, Klink and Gross (personal communication, 25 Feb 2014); correlations: \times Mulero et al. [25], --- parachor method. The statistical uncertainties of the simulation data indicate the standard error on a 95 % confidence interval.

$$\frac{\partial^{m+n} F / RT}{\partial^m (1/T) \partial^n (N/V)} \equiv A_{mn} = A_{mn}^i + A_{mn}^r, \quad (6)$$

wherein F is the Helmholtz energy, R the gas constant, T the temperature, N the number of particles and V the volume. The ideal part A_{mn}^i , which is needed to calculate any derivative of the Helmholtz energy, can be determined with other methods [33].

In order to extend this procedure, the present work deals with the usage of the microcanonical ensemble (NVE) to generate such data sets. In the NVE ensemble, the number of particles N , the Volume V and the total energy E of the system are kept constant. Although E is not directly accessible through experimental study, there are some advantages to using the NVE ensemble. Compared to other statistical mechanical ensembles, it is isolated from its environment in terms of energy or particle exchange and can therefore be considered as more stable and less susceptible to fluctuations. This implies that there is no need to regulate temperature through an external thermostat (NVT) and/or pressure through an external barostat (NpT) in molecular dynamics simulations, because E is conserved naturally through Newton's equations of motion. Moreover, the NVE ensemble links mechanics and thermodynamics in a very direct way [34].

In order to validate the implementation of the *NVE* ensemble into the simulation tool *ms2* [3], tests were carried out for the substance ethylene oxide using the molecular force field model by Eckl et al. [35]. As can be seen in figure 11, several simulations in the homogeneous fluid region were carried out using the *NVT* and *NVE* ensemble, respectively. It should be noted, that *NVT* ensemble simulations using this framework were compared to highly accurate equations of state in preceding work yielding excellent results. The overall agreement between the different types can be considered as quite good. Only in the vicinity of the critical point and for higher order derivatives, some deviations of the *NVE* ensemble simulation data were found. Contrary to the expectation of more stable molecular simulations in the *NVE* ensemble, the statistical uncertainties indicated by the error bars are quite similar. Therefore, further investigation is required.

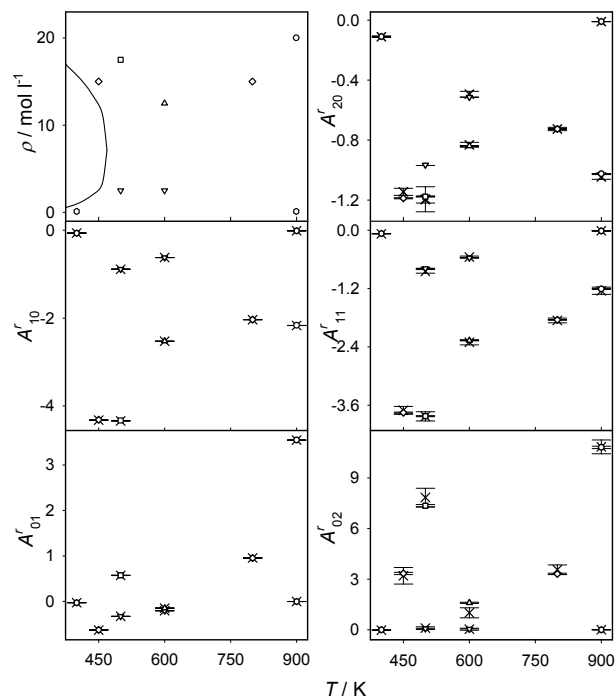


Fig. 11 Top left: Sampled state points of ethylene oxide in the temperature vs. density plane. Remaining figures: A_{1m}^r values as a function of temperature from Monte Carlo molecular simulation for ethylene oxide [35]. The open symbols denote various isochores in the *NVT* ensemble. The cross symbols represent the simulations which were carried out in the *NVE* ensemble.

6 Conclusion

Five new molecular models were developed and optimized in this work. They were validated against experimental data for the VLE properties, the critical point and second virial coefficient, showing a good coincidence with the reference data.

Interfacial simulations of a model fuel were carried out, yielding the surface tension for two binary mixtures, which agree well with the experimental reference data, and fill gaps where such data were unavailable.

The expected accuracy gain by using the microcanonical ensemble was not observed in the present simulations using the molecular simulation framework proposed by Lustig [33]. Here, further investigations are required.

7 Acknowledgements

We gratefully acknowledge support by Deutsche Forschungsgemeinschaft. This work was carried out under the auspices of the Boltzmann-Zuse Society (BZS) of Computational Molecular Engineering. The simulations were performed on the Cray XE6 (Hermit) at the High Performance Computing Center Stuttgart (HLRS).

References

- [1] B. Eckl, J. Vrabec, and H. Hasse. “Set of Molecular Models Based on Quantum Mechanical Ab Initio Calculations and Thermodynamic Data”. In: *J. Phys. Chem. B* 112 (2008), pp. 12710–12721.
- [2] M. W. Schmidt, K. K. Baldrige, J. A. Boatz, S. T. Elbert, M. S. Gordon, J. H. Jensen, S. Koseki, N. Matsunaga, K. A. Nguyen, S. Su, T. L. Windus, M. Dupuis, and J. A. Montgomery. “General atomic and molecular electronic structure system”. In: *J. Comput. Chem.* 14 (1993), pp. 1347–1363.
- [3] S. Deublein, B. Eckl, J. Stoll, S. V. Lishchuk, G. Guevara-Carrion, C. W. Glass, T. Merker, M. Bernreuther, H. Hasse, and J. Vrabec. “ms2: A molecular simulation tool for thermodynamic properties”. In: *Computer Physics Communications* 182 (2011), pp. 2350–2367.
- [4] T. Merker, J. Vrabec, and H. Hasse. “Engineering Molecular Models: Efficient Parameterization Procedure and Cyclohexanol as Case Study”. In: *Soft Mater.* 10 (2012), pp. 3–25.
- [5] R. L. Rowley, W. V. Wilding, J. L. Oscarson, Y. Yang, N. A. Zundel, T. E. Daubert, and R. P. Danner. *DIPPR data compilation of pure compound properties*. Design Institute for Physical Properties, AIChE. New York, 2006.
- [6] J. E. Jones. “On the Determination of Molecular Fields. I. From the Variation of the Viscosity of a Gas with Temperature”. In: *Proc. Roy. Soc.* 106A (1924), pp. 441–462.

- [7] J. E. Jones. "On the Determination of Molecular Fields. II. From the Equation of State of a Gas". In: *Proc. Roy. Soc.* 106A (1924), pp. 463–477.
- [8] M. P. Allen and D. J. Tildesley. *Computer simulations of liquids*. Oxford: Oxford University Press, 1987.
- [9] C. G. Gray and K. E. Gubbins. *Theory of molecular fluids*. Vol. 1. Fundamentals. Oxford: Clarendon Press, 1984.
- [10] R. S. Mulliken. "Criteria for the Construction of Good Self-Consistent-Field Molecular Orbital Wave Functions, and the Significance of LCAO-MO Population Analysis". In: *J. Chem. Phys.* 36 (2004), pp. 3428–3439.
- [11] H. A. Lorentz. "Über die Anwendung des Satzes vom Virial in der kinetischen Theorie der Gase". In: *Ann. Phys.* 12 (1881), pp. 127–136.
- [12] D. Berthelot. "Sur le Mélange des Gaz". In: *Compt. Rend. Ac. Sc.* 126 (1898), pp. 1703–1706.
- [13] G. Kamath, J. Robinson, and J. J. Potoff. "Application of TraPPE-UA force field for determination of vapor-liquid equilibria of carboxylate esters". In: *Fluid Phase Equilib.* 240 (2006), pp. 46–55.
- [14] R. L. Rowley, W. V. Wilding, J. L. Oscarson, Y. Yang, N. A. Zundel, T. E. Daubert, and R. P. Danner. *DIPPR Information and Data Evaluation Manager for the Design Institute for Physical Properties*. Design Institute for Physical Properties, AIChE. Version 5.0.2. New York, 2011.
- [15] *Dortmund Data Bank*. DDBST GmbH. Version 6.3.0.384. Oldenburg, 2010.
- [16] J. Stoll, J. Vrabec, and H. Hasse. "A set of molecular models for carbon monoxide and halogenated hydrocarbons". In: *J. Chem. Phys.* 119 (2003), pp. 11396–11407.
- [17] D.-Y. Peng and D. B. Robinson. "A New Two-Constant Equation of State". In: *Ind. Eng. Chem. Fund.* 15 (1976), pp. 59–64.
- [18] T. Ohta, H. Asano, and I. Nagata. "Thermodynamic Study of Complex-Formation in 4 Binary-Liquid Mixtures Containing Chloroform". In: *Fluid Phase Equilib.* 4 (1980), pp. 105–114.
- [19] J. Vrabec, J. Stoll, and H. Hasse. "A Set of Molecular Models for Symmetric Quadrupolar Fluids". In: *J. Phys. Chem. B* 105 (2001), pp. 12126–12133.
- [20] T. Windmann, M. Linnemann, and J. Vrabec. "Fluid Phase Behavior of Nitrogen + Acetone and Oxygen + Acetone by Molecular Simulation, Experiment and the Peng-Robinson Equation of State". In: *J. Chem. Eng. Data* 59 (2014), pp. 28–38.
- [21] C. Niethammer, M. Becker, M. Bernreuther, M. Buchholz, W. Eckhardt, A. Heinecke, S. Werth, H.-J. Bungartz, C. W. Glass, H. Hasse, J. Vrabec, and M. Horsch. "ls1 mardyn: The massively parallel molecular dynamics code for large systems". In: *J. Chem. Theory Comput.* 10 (2014), pp. 4455–4464.
- [22] J. Janeček. "Long Range Corrections in Inhomogeneous Simulations". In: *J. Phys. Chem. B* 110 (2006), pp. 6264–6269.
- [23] J. H. Irving and J. G. Kirkwood. "The Statistical Mechanical Theory of Transport Processes. IV. The Equations of Hydrodynamics". In: *J. Chem. Phys.* 18 (1950), pp. 817–829.

- [24] J.-C. Neyt, A. Wender, V. Lachet, and P. Malfreyt. “Prediction of the Temperature Dependence of the Surface Tension Of SO₂, N₂, O₂, and Ar by Monte Carlo Molecular Simulations”. In: *J. Phys. Chem. B* 115 (2011), pp. 9421–9430.
- [25] A. Mulero, I. Cachadiña, and M. I. Parra. “Recommended Correlations for the Surface Tension of Common Fluids”. In: *J. Phys. Chem. Ref. Data* 41 (2012), pp. 043105–1–043105–13.
- [26] Y. P. Blagoi, V. A. Kireev, M. P. Lobko, and V. V. Pashkov. “Surface Tension of Krypton, Methane, Deuteromethane and Oxygen”. In: *Ukr. Fiz. Zh.* 15 (1970), pp. 427–432.
- [27] V. B. Ostromoukhov and M. G. Ostronov. “Surface Tension of Liquid Solutions O₂–N₂ at 54–77 K”. In: *Zh. Fiz. Khim.* 68 (1994), pp. 39–43.
- [28] V. G. Baidakov, K. V. Khvostov, and G. N. Muratov. “Surface-Tension of Nitrogen, Oxygen and Methane in a wide Temperature-Range”. In: *Zh. Fiz. Khim.* 56 (1982), pp. 814–817.
- [29] Y. Sun and B. Y. Shekunov. “Surface tension of ethanol in supercritical CO₂”. In: *J. Supercrit. Fluid.* 27 (2003), pp. 73–83.
- [30] R. Schmidt and W. Wagner. “A new form of the equation of state for pure substances and its application to oxygen”. In: *Fluid Phase Equilib.* 19 (1985), pp. 175–200.
- [31] R. Span, E. W. Lemmon, R. T. Jacobsen, W. Wagner, and A. Yokozeki. “A Reference Equation of State for the Thermodynamic Properties of Nitrogen for Temperatures from 63.151 to 1000 K and Pressures to 2200 MPa”. In: *J. Phys. Chem. Ref. Data* 29 (2000), pp. 1361–1433.
- [32] S. Eckelsbach, S. Miroshnichenko, G. Rutkai, and J. Vrabec. “Surface tension, large scale thermodynamic data generation and vapor–liquid equilibria of real compounds”. In: *High Performance Computing in Science and Engineering '13*. Ed. by W. E. Nagel, D. H. Kröner, and M. M. Resch. Berlin: Springer, 2013, pp. 635–646.
- [33] R. Lustig. “Statistical analogues for fundamental equation of state derivatives”. In: *Mol. Phys.* 110 (2012), pp. 3041–3052.
- [34] R. Lustig. “Microcanonical Monte Carlo simulation of thermodynamic properties”. In: *J. Chem. Phys.* 109 (1998), pp. 8816–8828.
- [35] B. Eckl, J. Vrabec, and H. Hasse. “On the application of force fields for predicting a wide variety of properties: Ethylene oxide as an example”. In: *Fluid Phase Equilib.* 274 (2008), pp. 16–26.